Finite time Stability and Synchronization of the Glycolysis Reaction-Diffusion model

Raed Hatamleh[1], Issam Bendib[2], Ahmad Qazza[3], Rania Saadeh[3,*], Adel Ouannas[4], Mohamed Dalah[2]
[1]Department of Mathematics, Faculty of Science and Information Technology, Jadara University, P.O. Box 733, Irbid 21110, Jordan
[2]Applied Mathematics and Modeling Laboratory, Department of Mathematics, Faculty of Exact Sciences, Brothers Mentouri University of Constantine, Algeria
[3]Department of Mathematics, Faculty of Science, Zarqa University, Zarqa 13110, Jordan
[4]Department of Mathematics and Computer Science , University of Oum EL-Bouaghi, Oum El Bouaghi 04000, Algeria
Emails: raed@jadara.edu.jo; bendib.issam@doc.umc.edu.dz; aqazza@zu.edu.jo; rsaadeh@zu.edu.jo; ouannas.adel@univ-oeb.dz; dalah.mohamed@umc.edu.dz

Abstract

Finite-time stability is a critical property for systems where rapid stabilization is required, as it ensures that the system reaches and maintains equilibrium within a specified time frame, regardless of initial conditions. This contrasts with asymptotic stability, which only guarantees eventual convergence over an indefinite period. This research focuses on demonstrating the finite-time stability of the glycolysis reaction-diffusion system at its equilibrium point. The equilibrium points of the system are derived, and finite-time stability conditions are established. Definitions and lemmas are provided to support the theoretical framework, including conditions for finite-time convergence and Lyapunov stability. A key result shows that the system possesses a unique equilibrium point that can achieve finite-time stability under certain conditions. Additionally, the finite-time synchronization scheme is discussed, highlighting the process of rapidly achieving synchronized behavior in reaction-diffusion systems. The proposed method involves associating the main system with a response system and addressing synchronization discrepancies through the introduction of an error vector. This research provides a robust framework for understanding and achieving finite-time stability and synchronization in complex reaction-diffusion systems.

Keywords: Finite-time stability; Glycolysis reaction-diffusion system; Lyapunov stability; Finite-time synchronization scheme

1 Introduction

Glycolysis, a vital metabolic pathway in organisms, involves a series of biochemical reactions. Various theoretical frameworks have been proposed to accurately characterize the oscillatory patterns observed in glycolysis.[1,2] The Goldbeter model was intricately designed to explore the influence of spatial factors on glycolysis dynamics by integrating diffusion into reaction kinetics.[3] The extended spatial model, along with its modified version,[4] demonstrated a broad spectrum of spatiotemporal dynamics in glycolysis, ranging from propagating waves to spatiotemporal chaos, influenced by various initial conditions or substrate concentrations. These observed spatiotemporal patterns closely resemble the glycolytic waves observed in experimental setups.[5]

Recent advancements in mathematical modeling and numerical methods have significantly contributed to our understanding of complex systems like the glycolysis reaction-diffusion model. Abu-Ghuwaleh et al. introduced a novel approach in solving improper integrals, which plays a critical role in the analysis of such systems.[6] Similarly, Ahmed et al. developed the Conformable Double Laplace–Sumudu Iterative Method, which has proven effective in solving fractional differential equations, a key aspect in the study of reaction-diffusion systems.[7] The cubic B-spline method, as applied by Ala'yed et al., has shown to be an efficient tool for solving systems of Lane-Emden type equations, further enhancing the accuracy of numerical simulations in engineering applications.[8]

The study of chaotic systems has also seen significant progress, particularly in the context of fractional derivatives. Alzahrani et al. presented effective methods for the numerical analysis of chaotic circuits, which are applicable to the study of complex biochemical systems like glycolysis.[9] Additionally, the prediction and simulation of epidemics using fractional SEIR and ARIMA models, as explored by Alzahrani et al., highlight the potential of these methods in addressing real-world challenges.[10] Moreover, the use of advanced machine learning techniques, such as the physics-informed neural network method, has opened new avenues for predicting thermal distributions in complex systems, as demonstrated by Chandan et al.[11]

Furthermore, the development of new quadrature rules for n-times differentiable functions, as discussed by Hazaymeh et al., provides a robust framework for evaluating the stability and synchronization of reaction-diffusion systems.[12] The establishment of general formulas for integrals, as achieved by Saadeh et al., has been instrumental in refining the mathematical tools used in the analysis of these systems.[13] The adaptation of partial differential equations through the modified double ARA-Sumudu decomposition method, as shown by Saadeh et al., further underscores the importance of innovative mathematical approaches in this field.[14] Finally, the analytical solutions of coupled Hirota–Satsuma and KdV equations, as presented by Saadeh et al., offer valuable insights into the behavior of nonlinear systems, which are relevant to the study of glycolysis dynamics.[15]

Subsequently, researchers investigated the impact of feedback regulation of phosphofructokinase on the persistent spatiotemporal pattern of glycolytic oscillations in experiments conducted within an open spatial reactor.[16] This experimental setup served as inspiration for further exploration. Lavrova et al.[17] incorporated an inhomogeneous substrate influx into the Selkov model to account for the observed behaviors of waves in experiments. In this context, after several subsequent investigations,[18,19] the dynamic analysis of glycolytic wave propagation under non-uniform substrate supply conditions emerged as a practical model for understanding a fundamental aspect of energy metabolism.

Recognized by many, the phenomenon of ionic diffusion is prevalent, occurring as ions move through the cellular membrane. Consequently, it is crucial to account for the impact of diffusion on the overall system. This paper undertakes a fresh evaluation of the glycolysis reaction-diffusion system:[20,21]

$$\begin{cases} \frac{\partial \mathtt{U}_1(\mathfrak{r},\mathfrak{Z})}{\partial \mathfrak{Z}} = \mathfrak{d}_1 \Delta \mathtt{U}_1 + \mathfrak{b}\mathtt{U}_2 - \mathtt{U}_1 + \mathtt{U}_1^2\mathtt{U}_2, & \mathfrak{r} \in \Omega, \mathfrak{Z} > 0, \\ \frac{\partial \mathtt{U}_2(\mathfrak{r},\mathfrak{Z})}{\partial \mathfrak{Z}} = \mathfrak{d}_2 \Delta \mathtt{U}_2 + \mathfrak{a} - \mathfrak{b}\mathtt{U}_2 - \mathtt{U}_1^2\mathtt{U}_2, & \mathfrak{r} \in \Omega, \mathfrak{Z} > 0, \\ \frac{\partial \mathtt{U}_1}{\partial \eta} = \frac{\partial \mathtt{U}_2}{\partial \eta} = 0, & \mathfrak{r} \in \partial\Omega, \mathfrak{Z} > 0, \\ \mathtt{U}_1(\mathfrak{r},0) = \mathtt{U}_{1,0}(\mathfrak{r}) > 0, \quad \mathtt{U}_2(\mathfrak{r},0) = \mathtt{U}_{2,0}(\mathfrak{r}) > 0, & \mathfrak{r} \in \Omega, \end{cases} \tag{1}$$

In this context, Ω symbolizes a bounded region within the mathematical space $\mathbb{R}^n$ distinguished by a smooth boundary denoted by $\partial\Omega$, while Δ stands for the Laplace operator applied to Ω. Within the model, $\mathtt{U}_1$ and $\mathtt{U}_2$ denote the chemical concentrations, $\mathfrak{d}_1$ and $\mathfrak{d}_2$ represent diffusion coefficients, $\mathfrak{a}$ is the dimensionless input flow, and $\mathfrak{b}$ is the dimensionless constant rate for the low activity state.

Researchers from various fields have been intrigued by synchronization due to its potential applications across diverse scientific domains.[22] Understanding synchronization is essential for enhancing our comprehension of a wide range of real-world challenges relevant to disciplines such as chemistry, ecology, laser technology, biology, and cryptography.[23,24] Several types of synchronization have been suggested, encompassing finite-time synchronization, phase synchronization, anticipated synchronization, complete synchronization, lag synchronization, Q-S function synchronization, projective synchronization, and generalized synchronization.[25–35]

Finite-time synchronization of reaction-diffusion systems involves spatially extended systems governed by reaction-diffusion equations achieving synchronized behavior within a predetermined and finite time span. Unlike conventional synchronization methods, which can take an indefinite period to converge, finite-time synchronization ensures that the spatially distributed variables of the reaction-diffusion system synchronize within a specified time frame. This synchronization approach finds applications in fields like pattern formation, chemical kinetics, and biological modeling, where managing the temporal evolution of spatially extended systems is crucial.[35–45]

This study offers a novel perspective on investigating the stability of equilibrium points and synchronization within a specific subset of spatiotemporal partial differential systems within a finite time frame. The main objective is to explore both finite-time stability and finite-time synchronization within interconnected reaction-diffusion systems. By utilizing a Gronwall inequality to establish finite-time stable equilibrium points, we propose a linear control technique to achieve finite-time synchronization in glycolysis reaction-diffusion systems. To assess the effectiveness and feasibility of the proposed control methods, we analyze the synchronization behaviors of interconnected glycolysis systems.

The paper's structure is as follows: Section 2 focuses on finite-time stability results in the context of dynamical systems, particularly emphasizing achieving and maintaining system equilibrium within a specified duration. Unlike asymptotic stability, where equilibrium is approached over an indefinite period, finite-time stability ensures convergence within a predetermined time window, which is especially crucial in real-time control systems and critical applications. In Section 3, the focus is on a finite-time synchronization scheme applied to reaction-diffusion systems. The goal is to achieve synchronized behavior among components distributed across space within a specified timeframe. The equations describe the dynamics of the system components and introduce error vectors to quantify synchronization discrepancies. Linear controllers are identified to drive the error system solution towards zero as time approaches a specified threshold. Section 4 shifts from theoretical analysis to practical implementation through numerical simulations. The aim is to provide concrete examples that illustrate the theoretical concepts discussed earlier. MATLAB software and the finite difference method are employed for the simulations.

2 Finite time stability result

Finite-time stability emphasizes achieving and maintaining system equilibrium within a specified duration, regardless of initial conditions. In contrast to asymptotic stability, where equilibrium is gradually approached over an indefinite period, finite-time stability ensures convergence within a predetermined time window. This attribute is particularly valuable in real-time control systems and critical applications where rapid stabilization is paramount.

Furthermore, we discuss demonstrating the finite-time stability of the Glycolysis reaction-diffusion system at its equilibrium point. Initially, we determine the equilibrium points of the system (2), defined by the following equations:

$$\begin{cases} \mathfrak{d}_1 \Delta \mathtt{U}_1^* + \mathfrak{b}\mathtt{U}_2^* - \mathtt{U}_1^* + \mathtt{U}_1^{*2}\mathtt{U}_2^* = 0, \\ \mathfrak{d}_2 \Delta \mathtt{U}_2^* + \mathfrak{a} - \mathfrak{b}\mathtt{U}_2^* - \mathtt{U}_1^{*2}\mathtt{U}_2^* = 0, \end{cases} \tag{2}$$

Resulting in a unique equilibrium point for the system (2) given by:

$$(\mathtt{U}_1^*, \mathtt{U}_2^*) = \left(\mathfrak{a}, \frac{\mathfrak{a}}{\mathfrak{a}^2 + \mathfrak{b}} \right). \tag{3}$$

Definition 2.1. [46] Consider the nonlinear dynamical system (4)

$$\begin{cases} \mathtt{W}'(\mathfrak{Z}) = \mathtt{G}(\mathtt{W}(\mathfrak{Z})), \quad \mathfrak{Z} \in \mathcal{I}_{\mathtt{W}_0}, \\ \mathtt{W}(0) = \mathtt{W}_0. \end{cases} \tag{4}$$

where, for every $\mathfrak{Z} \in \mathcal{I}_{\mathtt{W}_0}, \mathtt{W}(\mathfrak{Z}) \in \mathcal{D} \subset \mathbb{R}^n, \mathcal{I}_{\mathtt{W}_0} \subset \overline{\mathbb{R}}_+$ is the maximal interval of existence of a solution $\mathtt{W}(\mathfrak{Z})$ of (4), $0 \in \mathcal{I}_{\mathtt{W}_0}$, $\mathcal{D}$ is an open set with $0 \in \mathcal{D}$, $\mathtt{G}(0) = 0$, and $\mathtt{G}(.)$ is continuous on $\mathcal{D}$. The zero solution $\mathtt{W}(\mathfrak{Z}) \equiv 0$ to (4) is finite-time stable if there exist an open neighborhood $\mathcal{N} \subseteq \mathcal{D}$ of the origin and a function $\mathfrak{Z}^* : \mathcal{N}^* \to (0, \infty)$, called the settling-time function, such that the following statements hold

- Finite-time convergence. For every $\mathtt{W} \in \mathcal{N}^*$, the continuously differentiable map $s^{\mathtt{W}}(\mathfrak{Z})$ is defined on $[0, \mathfrak{Z}^*(\mathtt{W}))$, $s^{\mathtt{W}}(\mathfrak{Z}) \in \mathcal{N}^*$ for all $\mathfrak{Z} \in [0, \mathfrak{Z}^*(\mathtt{W}))$, and $\lim_{\mathfrak{Z} \to \mathfrak{Z}^*(\mathtt{W})} s^{\mathtt{W}}(\mathfrak{Z}) = 0$.
- Lyapunov stability. For every $\varepsilon > 0$ there exist $\delta > 0$ such $\mathcal{B}_\delta(0) \subset \mathcal{N}$ and $\mathtt{W} \in \mathcal{B}^*_\delta(0), s^{\mathtt{W}}(\mathfrak{Z}) \in \mathcal{B}_\varepsilon(0)$ for all $\mathfrak{Z} \in [0, \mathfrak{Z}^*(\mathtt{W}))$.

The zero solution $\mathtt{W}(\mathfrak{Z}) \equiv 0$ of (4) is globally finite-time stable if it is finite-time stable with $\mathcal{N} = \mathcal{D} = \mathbb{R}^n$.

Definition 2.2. $(\mathtt{U}_1^*, \mathtt{U}_2^*)$ is called as the finite-time equilibrium point of the system (1) if there is a $\mathfrak{Z}^* > 0$, such that $(\mathtt{U}_1, \mathtt{U}_2) \neq (\mathtt{U}_1^*, \mathtt{U}_2^*)$, $(\mathfrak{r}, \mathfrak{Z}) \in \Omega \times [0, \mathfrak{Z}^*)$, and $(\mathtt{U}_1, \mathtt{U}_2) \equiv (\mathtt{U}_1^*, \mathtt{U}_2^*), \forall (\mathfrak{r}, \mathfrak{Z}) \in \Omega \times [\mathfrak{Z}^*, +\infty)$.

Definition 2.3. [47] The system given by (1) is finite-time stable with respect to $\{\delta, \varepsilon, \mathtt{J}\}, \delta < \varepsilon$, if $\|\Psi_{\mathtt{L}}\| < \delta$ and $\forall \mathfrak{Z} \in \mathtt{J}$, implies $\|\mathtt{L}(\mathfrak{Z})\| < \varepsilon, \forall \mathfrak{Z} \in \mathtt{J}$.

Lemma 2.4. [48] *System (1) possesses a single continuous solution, denoted as* $(\mathtt{U}_1, \mathtt{U}_2)$, *which is globally and continuously defined and bounded within the domain* $\Omega \times [0, +\infty)$. *Additionally, there exists a positive constant* $\mathtt{C} \in \mathbb{R}^+$ *such that:*

$$\mathtt{U}_1(\mathfrak{r}, \mathfrak{Z}), \mathtt{U}_2(\mathfrak{r}, \mathfrak{Z}) \leq \mathtt{C}, \tag{5}$$

Lemma 2.5. [49] *Let* $\Omega \subset \mathbb{R}^m$ *be a bounded domain with smooth boundary* $\partial\Omega$ *of class* $\mathcal{C}^2, \xi(\mathfrak{r}) \in H_0^1(\Omega)$ *is a real-valued function and* $\frac{\partial \xi(\mathfrak{r})}{\partial \eta}|_{\partial\Omega} = 0$. *Then*

$$\zeta \int_\Omega |\xi(\mathfrak{r})|^2 d\mathfrak{r} \leq \int_\Omega |\nabla \xi(\mathfrak{r})|^2 d\mathfrak{r}, \tag{6}$$

where ζ *is defined as a positive eigenvalue of the problem:*

$$\begin{cases} \zeta\xi - \Delta\xi = 0, & \mathfrak{r} \in \Omega, \\ \frac{\partial \xi(\mathfrak{r})}{\partial \eta} = 0, & \mathfrak{r} \in \partial\Omega. \end{cases} \tag{7}$$

Lemma 2.6. [38] *There exists a* $\mathtt{K} = \max\left\{\mathtt{K}_3^2, \mathtt{K}_2(\mathtt{K}_1 + \mathtt{K}_3)\right\} > 0$ *such that:*

$$|\mathtt{U}_1| \leq \mathtt{K}_1, |\mathtt{U}_2| \leq \mathtt{K}_2, |\mathtt{V}_1| \leq \mathtt{K}_3,$$

Thus, we have

$$\left|\mathtt{V}_1^2\mathtt{V}_2 - \mathtt{U}_1^2\mathtt{U}_2\right| \leq \mathtt{K}(|\mathtt{V}_1 - \mathtt{U}_1| + |\mathtt{V}_2 - \mathtt{U}_2|), \tag{8}$$

Lemma 2.7. [37, 40] ***(Gronwall inequality)*** *Assume that function* $\mathtt{Y}(\mathfrak{Z})$ *satisfies:*

$$\mathtt{Y}(\mathfrak{Z}) \leq \mathtt{F}_1(\mathfrak{Z}) + \int_0^{\mathfrak{Z}} \mathtt{Y}(\mathfrak{S})\mathtt{F}_2(\mathfrak{S}) d\mathfrak{S}, \quad \mathfrak{Z} \in [0, \mathfrak{Z}^*], \mathfrak{Z}^* < \infty, \tag{9}$$

where $\mathtt{Y}(\mathfrak{Z}), \mathtt{F}_1(\mathfrak{Z}), \mathtt{F}_2(\mathfrak{Z}) \in C[0, \mathfrak{Z}^*], \mathfrak{Z}^* < \infty$, *and* $\mathtt{F}_2(\mathfrak{Z}) \geq 0$. *If* $\mathtt{F}_1(\mathfrak{Z})$ *is non decreasing, then*

$$\mathtt{Y}(\mathfrak{Z}) < \mathtt{F}_1(\mathfrak{Z}) e^{\int_0^{\mathfrak{Z}} \mathtt{F}_2(\mathfrak{S}) d\mathfrak{S}}, \tag{10}$$

Theorem 2.8. *For the equilibrium point* $(\mathtt{U}_1^*, \mathtt{U}_2^*)$ *of system (1) to exhibit finite-time stability, it must satisfy the following condition:*

$$\max\left\{2\mathtt{K} + \frac{\mathfrak{b}}{2} - \mathfrak{d}_1\zeta_1 - 1, 2\mathtt{K} - \frac{\mathfrak{b}}{2} - \mathfrak{d}_2\zeta_2\right\} > 0, \tag{11}$$

Additionally, $\mathfrak{Z}_1^*$ *is defined as:*

$$\mathfrak{Z}_1^* = \frac{1}{2\max\left\{2\mathtt{K} + \frac{\mathfrak{b}}{2} - \mathfrak{d}_1\zeta_1 - 1, 2\mathtt{K} - \frac{\mathfrak{b}}{2} - \mathfrak{d}_2\zeta_2\right\}} \ln\left(\frac{\varepsilon}{\delta}\right). \tag{12}$$

Proof. Considering a positive Lyapunov function defined by:

$$\mathtt{L}^{*}\left(\mathfrak{Z}\right)=\frac{1}{2}\int_{\Omega}\left(\left(\mathtt{U}_{1}-\mathtt{U}_{1}^{*}\right)^{2}+\left(\mathtt{U}_{2}-\mathtt{U}_{2}^{*}\right)^{2}\right)\,d\mathfrak{r}, \tag{13}$$

By applying Green's formula, and Lemmas 2 and 3, we derive the following results:

$$\begin{aligned}
\frac{\partial \mathtt{L}^{*}\left(\mathfrak{Z}\right)}{\partial \mathfrak{Z}} &= \frac{1}{2}\int_{\Omega}\frac{\partial\left(\mathtt{U}_{1}-\mathtt{U}_{1}^{*}\right)^{2}}{\partial \mathfrak{Z}}\,d\mathfrak{r}+\frac{1}{2}\int_{\Omega}\frac{\partial\left(\mathtt{U}_{2}-\mathtt{U}_{2}^{*}\right)^{2}}{\partial \mathfrak{Z}}\,d\mathfrak{r}\\
&= \int_{\Omega}\left(\mathtt{U}_{1}-\mathtt{U}_{1}^{*}\right)\frac{\partial\left(\mathtt{U}_{1}-\mathtt{U}_{1}^{*}\right)}{\partial \mathfrak{Z}}\,d\mathfrak{r}+\int_{\Omega}\left(\mathtt{U}_{2}-\mathtt{U}_{2}^{*}\right)\frac{\partial\left(\mathtt{U}_{2}-\mathtt{U}_{2}^{*}\right)}{\partial \mathfrak{Z}}\,d\mathfrak{r}\\
&= \int_{\Omega}\left(\mathtt{U}_{1}-\mathtt{U}_{1}^{*}\right)\left(\frac{\partial \mathtt{U}_{1}}{\partial \mathfrak{Z}}-\frac{\partial \mathtt{U}_{1}^{*}}{\partial \mathfrak{Z}}\right)\,d\mathfrak{r}+\int_{\Omega}\left(\mathtt{U}_{2}-\mathtt{U}_{2}^{*}\right)\left(\frac{\partial \mathtt{U}_{2}}{\partial \mathfrak{Z}}-\frac{\partial \mathtt{U}_{2}^{*}}{\partial \mathfrak{Z}}\right)\,d\mathfrak{r}\\
&= \int_{\Omega}\left(\mathtt{U}_{1}-\mathtt{U}_{1}^{*}\right)\left[\mathfrak{d}_{1}\Delta\left(\mathtt{U}_{1}-\mathtt{U}_{1}^{*}\right)+\mathfrak{b}\left(\mathtt{U}_{2}-\mathtt{U}_{2}^{*}\right)-\left(\mathtt{U}_{1}-\mathtt{U}_{1}^{*}\right)+\mathtt{U}_{1}^{2}\mathtt{U}_{2}-\mathtt{U}_{1}^{*2}\mathtt{U}_{2}^{*}\right]\,d\mathfrak{r}\\
&+ \int_{\Omega}\left(\mathtt{U}_{2}-\mathtt{U}_{2}^{*}\right)\left[\mathfrak{d}_{2}\Delta\left(\mathtt{U}_{2}-\mathtt{U}_{2}^{*}\right)-\mathfrak{b}\left(\mathtt{U}_{2}-\mathtt{U}_{2}^{*}\right)-\mathtt{U}_{1}^{2}\mathtt{U}_{2}+\mathtt{U}_{1}^{*2}\mathtt{U}_{2}^{*}\right]\,d\mathfrak{r}\\
&= \mathfrak{d}_{1}\int_{\Omega}\left(\mathtt{U}_{1}-\mathtt{U}_{1}^{*}\right)\Delta\left(\mathtt{U}_{1}-\mathtt{U}_{1}^{*}\right)\,d\mathfrak{r}+\mathfrak{d}_{2}\int_{\Omega}\left(\mathtt{U}_{2}-\mathtt{U}_{2}^{*}\right)\Delta\left(\mathtt{U}_{2}-\mathtt{U}_{2}^{*}\right)\,d\mathfrak{r}+\mathfrak{b}\int_{\Omega}\left(\mathtt{U}_{1}-\mathtt{U}_{1}^{*}\right)\left(\mathtt{U}_{2}-\mathtt{U}_{2}^{*}\right)\,d\mathfrak{r}\\
&+ \int_{\Omega}\left(\left(\mathtt{U}_{1}-\mathtt{U}_{1}^{*}\right)-\left(\mathtt{U}_{2}-\mathtt{U}_{2}^{*}\right)\right)\left(\mathtt{U}_{1}^{2}\mathtt{U}_{2}-\mathtt{U}_{1}^{*2}\mathtt{U}_{2}^{*}\right)\,d\mathfrak{r}-\int_{\Omega}\left(\mathtt{U}_{1}-\mathtt{U}_{1}^{*}\right)^{2}\,d\mathfrak{r}-\mathfrak{b}\int_{\Omega}\left(\mathtt{U}_{2}-\mathtt{U}_{2}^{*}\right)^{2}\,d\mathfrak{r}\\
&\leq \mathfrak{d}_{1}\int_{\Omega}\left(\mathtt{U}_{1}-\mathtt{U}_{1}^{*}\right)\Delta\left(\mathtt{U}_{1}-\mathtt{U}_{1}^{*}\right)\,d\mathfrak{r}+\mathfrak{d}_{2}\int_{\Omega}\left(\mathtt{U}_{2}-\mathtt{U}_{2}^{*}\right)\Delta\left(\mathtt{U}_{2}-\mathtt{U}_{2}^{*}\right)\,d\mathfrak{r}+\mathfrak{b}\int_{\Omega}\left|\mathtt{U}_{1}-\mathtt{U}_{1}^{*}\right|\left|\mathtt{U}_{2}-\mathtt{U}_{2}^{*}\right|\,d\mathfrak{r}\\
&+ \int_{\Omega}\left(\left|\mathtt{U}_{1}-\mathtt{U}_{1}^{*}\right|+\left|\mathtt{U}_{2}-\mathtt{U}_{2}^{*}\right|\right)\left|\mathtt{U}_{1}^{2}\mathtt{U}_{2}-\mathtt{U}_{1}^{*2}\mathtt{U}_{2}^{*}\right|\,d\mathfrak{r}-\int_{\Omega}\left(\mathtt{U}_{1}-\mathtt{U}_{1}^{*}\right)^{2}\,d\mathfrak{r}-\mathfrak{b}\int_{\Omega}\left(\mathtt{U}_{2}-\mathtt{U}_{2}^{*}\right)^{2}\,d\mathfrak{r}\\
&\leq -\mathfrak{d}_{1}\int_{\Omega}\left|\nabla\left(\mathtt{U}_{1}-\mathtt{U}_{1}^{*}\right)\right|^{2}\,d\mathfrak{r}-\mathfrak{d}_{2}\int_{\Omega}\left|\nabla\left(\mathtt{U}_{2}-\mathtt{U}_{2}^{*}\right)\right|^{2}\,d\mathfrak{r}+\frac{\mathfrak{b}}{2}\int_{\Omega}\left(\left(\mathtt{U}_{1}-\mathtt{U}_{1}^{*}\right)^{2}+\left(\mathtt{U}_{2}-\mathtt{U}_{2}^{*}\right)^{2}\right)\,d\mathfrak{r}\\
&+ 2\mathtt{K}\int_{\Omega}\left(\left(\mathtt{U}_{1}-\mathtt{U}_{1}^{*}\right)^{2}+\left(\mathtt{U}_{2}-\mathtt{U}_{2}^{*}\right)^{2}\right)\,d\mathfrak{r}-\int_{\Omega}\left(\mathtt{U}_{1}-\mathtt{U}_{1}^{*}\right)^{2}\,d\mathfrak{r}-\mathfrak{b}\int_{\Omega}\left(\mathtt{U}_{2}-\mathtt{U}_{2}^{*}\right)^{2}\,d\mathfrak{r}\\
&\leq \left(2\mathtt{K}+\frac{\mathfrak{b}}{2}-\mathfrak{d}_{1}\zeta_{1}-1\right)\int_{\Omega}\left(\mathtt{U}_{1}-\mathtt{U}_{1}^{*}\right)^{2}\,d\mathfrak{r}+\left(2\mathtt{K}-\frac{\mathfrak{b}}{2}-\mathfrak{d}_{2}\zeta_{2}\right)\int_{\Omega}\left(\mathtt{U}_{2}-\mathtt{U}_{2}^{*}\right)^{2}\,d\mathfrak{r}\\
&\leq 2\max\left\{2\mathtt{K}+\frac{\mathfrak{b}}{2}-\mathfrak{d}_{1}\zeta_{1}-1,2\mathtt{K}-\frac{\mathfrak{b}}{2}-\mathfrak{d}_{2}\zeta_{2}\right\}\mathtt{L}^{*}\left(\mathfrak{Z}\right).
\end{aligned} \tag{14}$$

Assume

$$\max\left\{2\mathtt{K}+\frac{\mathfrak{b}}{2}-\mathfrak{d}_{1}\zeta_{1}-1,2\mathtt{K}-\frac{\mathfrak{b}}{2}-\mathfrak{d}_{2}\zeta_{2}\right\}>0,$$

Then,

$$\mathtt{L}^{*}\left(\mathfrak{Z}\right)\leq \mathtt{L}^{*}\left(0\right)+2\max\left\{2\mathtt{K}+\frac{\mathfrak{b}}{2}-\mathfrak{d}_{1}\zeta_{1}-1,2\mathtt{K}-\frac{\mathfrak{b}}{2}-\mathfrak{d}_{2}\zeta_{2}\right\}\int_{0}^{\mathfrak{Z}}\mathtt{L}^{*}\left(\mathfrak{S}\right)\,d\mathfrak{S}. \tag{15}$$

In accordance with Lemma 4, this results in the conclusion that:

$$\mathtt{L}^{*}\left(\mathfrak{Z}\right)\leq \mathtt{L}^{*}\left(0\right)e^{2\max\left\{2\mathtt{K}+\frac{\mathfrak{b}}{2}-\mathfrak{d}_{1}\zeta_{1}-1,2\mathtt{K}-\frac{\mathfrak{b}}{2}-\mathfrak{d}_{2}\zeta_{2}\right\}\mathfrak{Z}}, \tag{16}$$

We can additionally infer:

$$\begin{aligned}\left\|\mathtt{L}^{*}\left(\mathfrak{Z}\right)\right\| &\leq \left\|\mathtt{L}^{*}\left(0\right)\right\| \left\| e^{2\max\left\{2\mathtt{K}+\frac{\mathfrak{b}}{2}-\mathfrak{d}_1\zeta_1-1,2\mathtt{K}-\frac{\mathfrak{b}}{2}-\mathfrak{d}_2\zeta_2\right\}\mathfrak{Z}}\right\| \\ &\leq F\left(\mathfrak{Z}\right)=\delta e^{2\max\left\{2\mathtt{K}+\frac{\mathfrak{b}}{2}-\mathfrak{d}_1\zeta_1-1,2\mathtt{K}-\frac{\mathfrak{b}}{2}-\mathfrak{d}_2\zeta_2\right\}\mathfrak{Z}},\end{aligned} \tag{17}$$

Alternatively, the setting time can be defined as:

$$\mathfrak{Z}_1^{*}=\frac{1}{2\max\left\{2\mathtt{K}+\frac{\mathfrak{b}}{2}-\mathfrak{d}_1\zeta_1-1,2\mathtt{K}-\frac{\mathfrak{b}}{2}-\mathfrak{d}_2\zeta_2\right\}}\ln\left(\frac{\varepsilon}{\delta}\right), \tag{18}$$

According to Definitions 2 and 3, it can be inferred that the system (1) demonstrates stability within a finite time frame, provided that $\mathfrak{Z}$ remains equal to or greater than $\mathfrak{Z}^{*}$.

3 Finite-time synchronization scheme

Finite-time synchronization in reaction-diffusion systems refers to the process of quickly achieving synchronized behavior among components that are distributed across space within a specified duration. The goal is to rapidly establish coherence across different spatial dimensions within the system's elements. It's important to highlight that the main system (1) can be associated with a subsequent response system to aid in this synchronization process, as illustrated by the following equations:

$$\begin{cases}\frac{\partial \mathtt{V}_1(\mathfrak{r},\mathfrak{Z})}{\partial \mathfrak{Z}}=\mathfrak{d}_1\Delta\mathtt{V}_1+\mathfrak{b}\mathtt{V}_2-\mathtt{V}_1+\mathtt{V}_1^2\mathtt{V}_2+\mathtt{C}_1, & \mathfrak{r}\in\Omega,\mathfrak{Z}>0,\\ \frac{\partial \mathtt{V}_2(\mathfrak{r},\mathfrak{Z})}{\partial \mathfrak{Z}}=\mathfrak{d}_2\Delta\mathtt{V}_2+\mathfrak{a}-\mathfrak{b}\mathtt{V}_2-\mathtt{V}_1^2\mathtt{V}_2+\mathtt{C}_2, & \mathfrak{r}\in\Omega,\mathfrak{Z}>0,\\ \frac{\partial \mathtt{V}_1}{\partial \eta}=\frac{\partial \mathtt{V}_2}{\partial \eta}=0, & \mathfrak{r}\in\partial\Omega,\mathfrak{Z}>0,\\ \mathtt{V}_1\left(\mathfrak{r},0\right)=\mathtt{V}_{1,0}\left(\mathfrak{r}\right)>0, & \mathtt{V}_2\left(\mathfrak{r},0\right)=\mathtt{V}_{2,0}\left(\mathfrak{r}\right)>0,\quad \mathfrak{r}\in\Omega,\end{cases} \tag{19}$$

To address synchronization discrepancies between equations (1) and (19), we introduce the error vector $\mathtt{e}\left(\mathfrak{r},\mathfrak{Z}\right)$, defined as:

$$\mathtt{e}\left(\mathfrak{r},\mathfrak{Z}\right)=\begin{pmatrix}\mathtt{e}_1\\ \mathtt{e}_2\end{pmatrix}=\begin{pmatrix}\mathtt{V}_1-\mathtt{U}_1\\ \mathtt{V}_2-\mathtt{U}_2\end{pmatrix}. \tag{20}$$

In the subsequent analysis, we identify the linear controllers $\mathtt{C}_1$ and $\mathtt{C}_2$, which drive the error system solution towards zero as $\mathfrak{Z}$ approaches $\mathfrak{Z}^{*}$. Our objective is to demonstrate that the discrepancy diminishes to zero as time converges to $\mathfrak{Z}^{*}$. This can be achieved by substituting the expression derived from equation (1) into the error system described in equation (21):

$$\begin{cases}\frac{\partial \mathtt{e}_1(\mathfrak{r},\mathfrak{Z})}{\partial \mathfrak{Z}}=\mathfrak{d}_1\Delta\mathtt{e}_1+\mathfrak{b}\mathtt{e}_2-\mathtt{e}_1+\mathtt{V}_1^2\mathtt{V}_2-\mathtt{U}_1^2\mathtt{U}_2+\mathtt{C}_1, & \mathfrak{r}\in\Omega,\mathfrak{Z}>0,\\ \frac{\partial \mathtt{e}_2(\mathfrak{r},\mathfrak{Z})}{\partial \mathfrak{Z}}=\mathfrak{d}_2\Delta\mathtt{e}_2-\mathfrak{b}\mathtt{e}_2-\mathtt{V}_1^2\mathtt{V}_2+\mathtt{U}_1^2\mathtt{U}_2+\mathtt{C}_2, & \mathfrak{r}\in\Omega,\mathfrak{Z}>0,\\ \frac{\partial \mathtt{e}_1}{\partial \eta}=\frac{\partial \mathtt{e}_2}{\partial \eta}=0, & \mathfrak{r}\in\partial\Omega,\mathfrak{Z}>0,\\ \mathtt{e}_1\left(\mathfrak{r},0\right)=\mathtt{e}_{1,0}\left(\mathfrak{r}\right)>0, & \mathtt{e}_2\left(\mathfrak{r},0\right)=\mathtt{e}_{2,0}\left(\mathfrak{r}\right)>0,\quad \mathfrak{r}\in\Omega.\end{cases} \tag{21}$$

Theorem 3.1. [41] $(\mathtt{e}_1^*, \mathtt{e}_2^*)$ *is a finite-time stability equilibrium point of the nonlinear system (21) if there exists a positive definite Lyapunov function* $\mathtt{L} : [0, +\infty) \times \Omega \to \mathbb{R}_+$, *three class* $\mathcal{K}$ *functions* η, β, Λ, *and a* $\delta > 0$ *such that*

- $\eta \left\| \mathtt{e} \left(\mathfrak{Z} \right) \right\| \leq \mathtt{L} \left(\mathfrak{Z}, \mathtt{e} \left(\mathfrak{Z} \right) \right) \leq \beta \left\| \mathtt{e} \left(\mathfrak{Z} \right) \right\|,$
- $\frac{\partial \mathtt{L}(\mathfrak{Z}, \mathtt{e}(\mathfrak{Z}))}{\partial \mathfrak{Z}} < -\Lambda \mathtt{L} \left(\mathfrak{Z}, \mathtt{e} \left(\mathfrak{Z} \right) \right),$
- $\int_0^{\varepsilon} \frac{d\mathtt{e}}{\Lambda(\mathtt{e})} < +\infty, (\forall \varepsilon : 0 < \varepsilon \leq \delta).$

Definition 3.2. [42, 43] If there exists a setting time $\mathfrak{Z}^* > 0$ such that

$$\lim_{\mathfrak{Z} \to \mathfrak{Z}^*} \left\| \mathtt{e}_1 \left(\mathfrak{Z} \right) \right\| + \left\| \mathtt{e}_2 \left(\mathfrak{Z} \right) \right\| = 0, \tag{22}$$

and

$$\left\| \mathtt{e}_1 \left(\mathfrak{Z} \right) \right\| + \left\| \mathtt{e}_2 \left(\mathfrak{Z} \right) \right\| \equiv 0, \quad \forall \mathfrak{Z} \geq \mathfrak{Z}^*, \tag{23}$$

then the derive-response systems (1) and (19) are synchronized in finite time.

Theorem 3.3. *The derived-response systems, as described by equations (1) and (19), can attain stable and synchronized states within a finite duration under the condition that the parameter* $\mathfrak{Z}^*$ *satisfies:*

$$\mathfrak{Z}_2^* = \frac{\mathtt{L}\left(0\right)}{2 \min \left\{ 1 + \mathfrak{d}_1 \zeta_1, \mathfrak{b} + \mathfrak{d}_2 \zeta_2 \right\} \mathtt{L} \left(\mathfrak{Z}_{\max} \right)}, \tag{24}$$

This achievement is facilitated by employing a two-dimensional linear control law given by:

$$\begin{cases} \mathtt{C}_1 = -2\mathtt{K}\mathtt{e}_1 - \mathfrak{b}\mathtt{e}_2, \\ \mathtt{C}_2 = -2\mathtt{K}\mathtt{e}_2. \end{cases} \tag{25}$$

Prof. Using the control law, we define the expression of the error system as follows:

$$\begin{cases} \frac{\partial \mathtt{e}_1(\mathfrak{r}, \mathfrak{Z})}{\partial \mathfrak{Z}} = \mathfrak{d}_1 \Delta \mathtt{e}_1 - (1 + 2\mathtt{K})\, \mathtt{e}_1 + \mathtt{V}_1^2 \mathtt{V}_2 - \mathtt{U}_1^2 \mathtt{U}_2, & \mathfrak{r} \in \Omega, \mathfrak{Z} > 0, \\ \frac{\partial \mathtt{e}_2(\mathfrak{r}, \mathfrak{Z})}{\partial \mathfrak{Z}} = \mathfrak{d}_2 \Delta \mathtt{e}_2 - (\mathfrak{b} + 2\mathtt{K})\, \mathtt{e}_2 - \mathtt{V}_1^2 \mathtt{V}_2 + \mathtt{U}_1^2 \mathtt{U}_2, & \mathfrak{r} \in \Omega, \mathfrak{Z} > 0, \\ \frac{\partial \mathtt{e}_1}{\partial \eta} = \frac{\partial \mathtt{e}_2}{\partial \eta} = 0, & \mathfrak{r} \in \partial\Omega, \mathfrak{Z} > 0, \\ \mathtt{e}_1 \left(\mathfrak{r}, 0 \right) = \mathtt{e}_{1,0} \left(\mathfrak{r} \right) > 0, \quad \mathtt{e}_2 \left(\mathfrak{r}, 0 \right) = \mathtt{e}_{2,0} \left(\mathfrak{r} \right) > 0, & \mathfrak{r} \in \Omega, \end{cases} \tag{26}$$

Here, the function $\mathtt{L}$ is defined as:

$$\mathtt{L} \left(\mathfrak{Z} \right) = \frac{1}{2} \int_{\Omega} \left(\mathtt{e}_1^2 + \mathtt{e}_2^2 \right) \, d\mathfrak{r}, \tag{27}$$

To compute $\frac{\partial \mathtt{L}}{\partial \mathfrak{Z}}$ using Lemma 2-3, we proceed as follows:

$$\begin{aligned}
\frac{\partial \mathtt{L}(\mathfrak{Z})}{\partial \mathfrak{Z}} &= \frac{1}{2}\int_{\Omega}\frac{\partial \mathtt{e}_1^2}{\partial \mathfrak{Z}}\,d\mathfrak{r} + \frac{1}{2}\int_{\Omega}\frac{\partial \mathtt{e}_2^2}{\partial \mathfrak{Z}}\,d\mathfrak{r} \\
&= \int_{\Omega}\mathtt{e}_1\frac{\partial \mathtt{e}_1}{\partial \mathfrak{Z}}\,d\mathfrak{r} + \int_{\Omega}\mathtt{e}_2\frac{\partial \mathtt{e}_2}{\partial \mathfrak{Z}}\,d\mathfrak{r} \\
&= \int_{\Omega}\mathtt{e}_1\left[\mathfrak{d}_1\Delta\mathtt{e}_1 - (1+2\mathtt{K})\,\mathtt{e}_1 + \mathtt{V}_1^2\mathtt{V}_2 - \mathtt{U}_1^2\mathtt{U}_2\right]\,d\mathfrak{r} + \int_{\Omega}\mathtt{e}_2\left[\mathfrak{d}_2\Delta\mathtt{e}_2 - (\mathfrak{b}+2\mathtt{K})\,\mathtt{e}_2 - \mathtt{V}_1^2\mathtt{V}_2 + \mathtt{U}_1^2\mathtt{U}_2\right]\,d\mathfrak{r} \\
&\leq -\mathfrak{d}_1\int_{\Omega}\left|\nabla\mathtt{e}_1\right|^2\,d\mathfrak{r} - \mathfrak{d}_2\int_{\Omega}\left|\nabla\mathtt{e}_2\right|^2\,d\mathfrak{r} - (1+2\mathtt{K})\int_{\Omega}\mathtt{e}_1^2\,d\mathfrak{r} - (\mathfrak{b}+2\mathtt{K})\int_{\Omega}\mathtt{e}_2^2\,d\mathfrak{r} + \mathtt{K}\int_{\Omega}\left(|\mathtt{e}_1|+|\mathtt{e}_1|\right)^2\,d\mathfrak{r} \\
&\leq -\mathfrak{d}_1\int_{\Omega}\left|\nabla\mathtt{e}_1\right|^2\,d\mathfrak{r} - \mathfrak{d}_2\int_{\Omega}\left|\nabla\mathtt{e}_2\right|^2\,d\mathfrak{r} - (1+2\mathtt{K})\int_{\Omega}\mathtt{e}_1^2\,d\mathfrak{r} - (\mathfrak{b}+2\mathtt{K})\int_{\Omega}\mathtt{e}_2^2\,d\mathfrak{r} + 2\mathtt{K}\int_{\Omega}\left(|\mathtt{e}_1|^2+|\mathtt{e}_1|^2\right)\,d\mathfrak{r} \\
&\leq -\left(1+\mathfrak{d}_1\zeta_1\right)\int_{\Omega}\mathtt{e}_1^2\,d\mathfrak{r} - \left(\mathfrak{b}+\mathfrak{d}_2\zeta_2\right)\int_{\Omega}\mathtt{e}_2^2\,d\mathfrak{r} \\
&\leq -2\min\left\{1+\mathfrak{d}_1\zeta_1, \mathfrak{b}+\mathfrak{d}_2\zeta_2\right\}\mathtt{L}(\mathfrak{Z}).
\end{aligned} \tag{28}$$

Considering $\Lambda = 2\min\left\{1+\mathfrak{d}_1\zeta_1, \mathfrak{b}+\mathfrak{d}_2\zeta_2\right\}$, we can derive:

$$\int_0^{\varepsilon}\frac{1}{\Lambda}\,d\mathfrak{S} = \frac{\varepsilon}{2\min\left\{1+\mathfrak{d}_1\zeta_1, \mathfrak{b}+\mathfrak{d}_2\zeta_2\right\}} < +\infty, \tag{29}$$

By employing Theorem 2, we confirm that the absence of a solution in the error system (21) indicates stability within a finite period for the equilibrium point $(\mathtt{e}_1^*, \mathtt{e}_2^*) = (0,0)$. This suggests that the discrepancy between the derived and response systems diminishes to zero over a finite duration, signifying the achievement of synchronized behavior. Furthermore, the function $\mathtt{L}(\mathfrak{Z})$ decreases while remaining positive for $0 \leq \mathfrak{Z} < \mathfrak{Z}_2^* \leq \mathfrak{Z}_{\max}$. This indicates that as $\mathfrak{Z}$ increases, the value of $\mathtt{L}(\mathfrak{Z})$ decreases. Consequently, we have $\mathtt{L}(\mathfrak{Z}) \geq \mathtt{L}(\mathfrak{Z}_{\max})$. Additionally,

$$\begin{aligned}
\mathtt{L}(\mathfrak{Z}) &\leq \mathtt{L}(0) - 2\min\left\{1+\mathfrak{d}_1\zeta_1, \mathfrak{b}+\mathfrak{d}_2\zeta_2\right\}\int_0^{\mathfrak{Z}}\mathtt{L}(\mathfrak{S})\,d\mathfrak{S} \\
&\leq \mathtt{L}(0) - 2\min\left\{1+\mathfrak{d}_1\zeta_1, \mathfrak{b}+\mathfrak{d}_2\zeta_2\right\}\int_0^{\mathfrak{Z}}\mathtt{L}(\mathfrak{Z}_{\max})\,d\mathfrak{S} \\
&= \mathtt{L}(0) - 2\min\left\{1+\mathfrak{d}_1\zeta_1, \mathfrak{b}+\mathfrak{d}_2\zeta_2\right\}\mathtt{L}(\mathfrak{Z}_{\max})\,\mathfrak{Z}.
\end{aligned} \tag{30}$$

As $\mathfrak{Z}$ approaches $\mathfrak{Z}_2^*$, as per Definition 4, the function $\mathtt{L}$ tends to 0. Consequently,

$$\lim_{\mathfrak{Z}\to\mathfrak{Z}_2^*}\mathtt{L}(\mathfrak{Z}) \leq \mathtt{L}(0) - 2\min\left\{1+\mathfrak{d}_1\zeta_1, \mathfrak{b}+\mathfrak{d}_2\zeta_2\right\}\mathtt{L}(\mathfrak{Z}_{\max})\,\mathfrak{Z}_2^* = 0, \tag{31}$$

leading to the conclusion that

$$\mathfrak{Z}_2^* = \frac{\mathtt{L}(0)}{2\min\left\{1+\mathfrak{d}_1\zeta_1, \mathfrak{b}+\mathfrak{d}_2\zeta_2\right\}\mathtt{L}(\mathfrak{Z}_{\max})},$$

Based on the conditions delineated in Definition 4, the systems denoted as derived-response systems (1) and (19) exhibit the capacity to attain synchronization within a finite timeframe. Put differently, the behaviors of these systems, regulated by precise mathematical equations and conditions, converge towards a synchronized state within a specified interval. This synchronization represents a coveted outcome within the ambit of the ongoing study or analysis, indicating that the dynamics of the systems harmonize over time, thereby accomplishing the objective of fostering coherence or coordination among their constituent components or elements.

4 Numerical examples

The finite difference method is indispensable for modeling the Glycolysis Reaction-Diffusion system, yielding outstanding results. Through the discretization of both spatial and temporal domains, this computational technique effectively approximates the system's partial differential equations, capturing its intricate spatiotemporal dynamics. It enables the precise computation of concentration profiles and the temporal evolution of chemical species involved in glycolysis. Additionally, the method accurately represents diffusion and enzymatic kinetics within the spatial domain. Moreover, its flexible grid resolution allows researchers to balance computational accuracy and efficiency, thereby capturing finer details of the system's behavior. Essentially, the finite difference method serves as a powerful tool for exploring the complex dynamics of glycolysis, providing reliable insights into biochemical processes. This section presents practical simulations designed to illustrate the theoretical principles discussed earlier. These simulations were conducted using the finite difference method and MATLAB software. The section includes two illustrative examples:

Example 1. *Let* $\Omega = [0, 10]$ *and* $\mathfrak{Z} \in [0, 5]$. *We consider the following parameters:*

Variable	*Value*
$\mathfrak{d}_1$	0.5
$\mathfrak{d}_2$	0.75
$\mathfrak{a}$	0.2
$\mathfrak{b}$	0.4108075
$\mathtt{K}$	0.1996
ζ_1	0.15
ζ_2	0.15
δ	1
ε	2.25465
$\mathbb{N}$	50

The initial conditions are given by:

$$\mathtt{U}_{1,0}(\mathfrak{r}) = 0.25, \tag{32}$$
$$\mathtt{U}_{2,0}(\mathfrak{r}) = 0.25, \tag{33}$$

The conditions of Theorem 1 are met:

$$\max\left\{2\mathtt{K} + \frac{\mathfrak{b}}{2} - \mathfrak{d}_1\zeta_1 - 1, 2\mathtt{K} - \frac{\mathfrak{b}}{2} - \mathfrak{d}_2\zeta_2\right\} = 0.0813, \tag{34}$$

and

$$\mathfrak{Z}_1^* = \frac{1}{2\max\left\{2\mathtt{K} + \frac{\mathfrak{b}}{2} - \mathfrak{d}_1\zeta_1 - 1, 2\mathtt{K} - \frac{\mathfrak{b}}{2} - \mathfrak{d}_2\zeta_2\right\}} \ln\left(\frac{\varepsilon}{\delta}\right) = 5\ s. \tag{35}$$

The temporal and spatial solutions of system (1) with homogeneous Neumann boundary conditions are displayed in Figures 1 and 2. Theorem 1 states that system (1) exhibits finite-time stability at the equilibrium point $(\mathtt{U}_1^*, \mathtt{U}_2^*) = (0.2, 0.4436)$. *To confirm this numerically, the temporal and spatial solutions, along with errors, are depicted in Figure 2, focusing on one-dimensional space. This illustration provides conclusive evidence that the errors decrease to 0 as* $\mathfrak{Z}$ *approaches* $\mathfrak{Z}_1^* = 5$ *seconds (see Figure 3).*

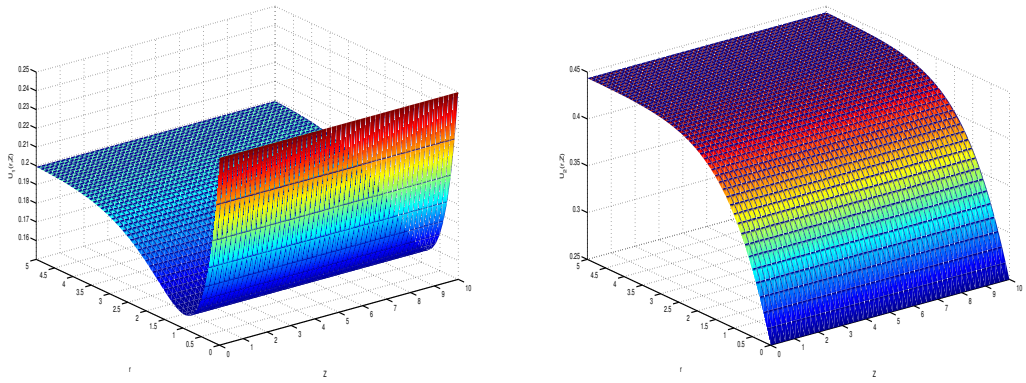

Figure 1: Dynamics behavior of solutions $\mathtt{U}_1\,(\mathfrak{r},\mathfrak{Z})$ and $\mathtt{U}_2\,(\mathfrak{r},\mathfrak{Z})$

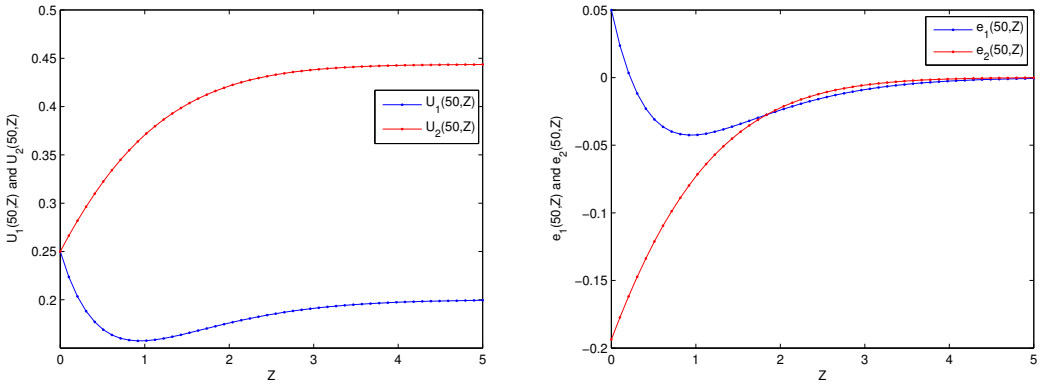

Figure 2: The state trajectories of the solutions $\mathtt{U}_1(50,\mathfrak{Z})$, $\mathtt{U}_2(50,\mathfrak{Z})$, $\mathtt{e}_1(50,\mathfrak{Z})$, and $\mathtt{e}_2(50,\mathfrak{Z})$ in 2D

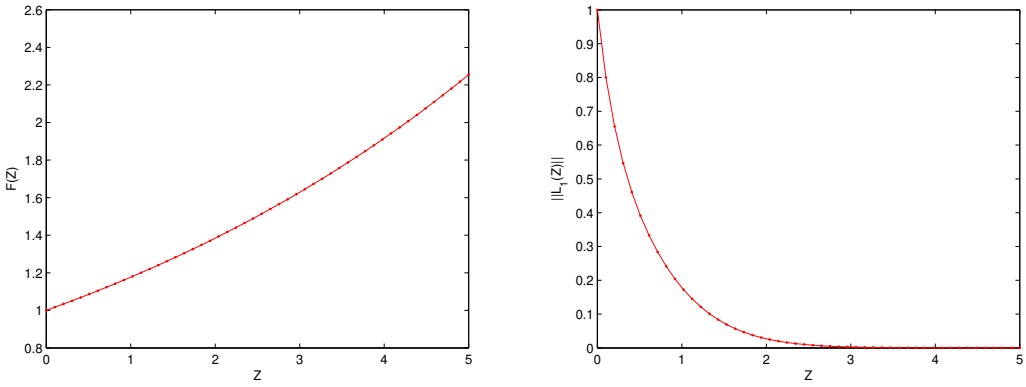

Figure 3: Estimation of the Lyapunov function $\|\mathtt{L}^*(\mathfrak{Z})\|$ and $F(\mathfrak{Z})$

Example 2. *Examine the domain* Ω *spanning the interval* $[0,6]$*, with* $\mathfrak{Z}$ *varying across the range of* $[0,100]$.

Variable	*Value*
$\mathfrak{d}_1$	10
$\mathfrak{d}_2$	10
$\mathfrak{a}$	1.75
$\mathfrak{b}$	1
$\mathtt{K}$	6.68
ζ_1	10
ζ_2	10
$\mathbb{N}$	50

Now, we establish the starting parameters for the derived-response systems (1) and (19) in the following manner:

$$\mathtt{U}_{1,0}(\mathfrak{r}) = 1, \tag{36}$$
$$\mathtt{U}_{2,0}(\mathfrak{r}) = 0.5, \tag{37}$$

and

$$\mathtt{V}_{1,0}(\mathfrak{r}) = 1.5, \tag{38}$$
$$\mathtt{V}_{2,0}(\mathfrak{r}) = 1. \tag{39}$$

We intend to create two controllers according to Theorem 3, referred to as $\mathtt{C}_1$ *and* $\mathtt{C}_2$*, respectively:*

$$\begin{cases} \mathtt{C}_1 = -13.36\mathtt{e}_1 - \mathtt{e}_2, \\ \mathtt{C}_2 = -13.36\mathtt{e}_2, \end{cases} \tag{40}$$

We find

$$\mathtt{L}(0) = 12.5000, \tag{41}$$
$$\mathtt{L}(5) = 6.1902 \times 10^{-4}, \tag{42}$$
$$\min\left\{1 + \mathfrak{d}_1\zeta_1, \mathfrak{b} + \mathfrak{d}_2\zeta_2\right\} = 101, \tag{43}$$

and

$$\mathfrak{Z}_2^* = \frac{\mathtt{L}(0)}{2\min\left\{1 + \mathfrak{d}_1\zeta_1, \mathfrak{b} + \mathfrak{d}_2\zeta_2\right\}\mathtt{L}(5)} = 99.9664s, \tag{44}$$

Figures 4-5 display the spatiotemporal evolution of systems (1) and (19), providing further insights in both 2-dimensional space (Figs. 4-5) and 7-dimensional space. Through numerical simulations, we illustrate the spatiotemporal solutions of the error synchronization system (21) in Figs. 5-6. This development strongly indicates the convergence of errors to 0 as $\mathfrak{Z}$ *approaches* $\mathfrak{Z}_2^* = 99.9664$ *s, allowing for the observation of finite-time behavior. Moreover, Fig. 8 clearly demonstrates the occurrence within the finite-time interval* $\mathfrak{Z}_2^* = 99.9664$ *s.*

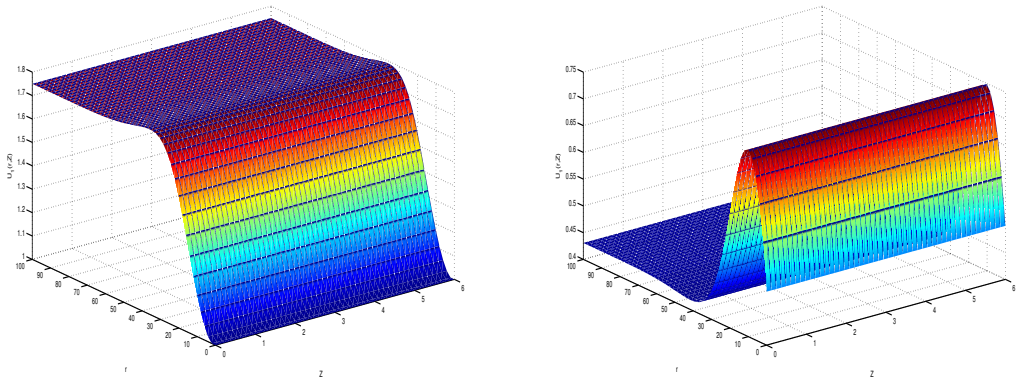

Figure 4: Dynamic behavior of the master system (1) $\mathtt{U}_1(\mathfrak{r},\mathfrak{Z})$ and $\mathtt{U}_2(\mathfrak{r},\mathfrak{Z})$

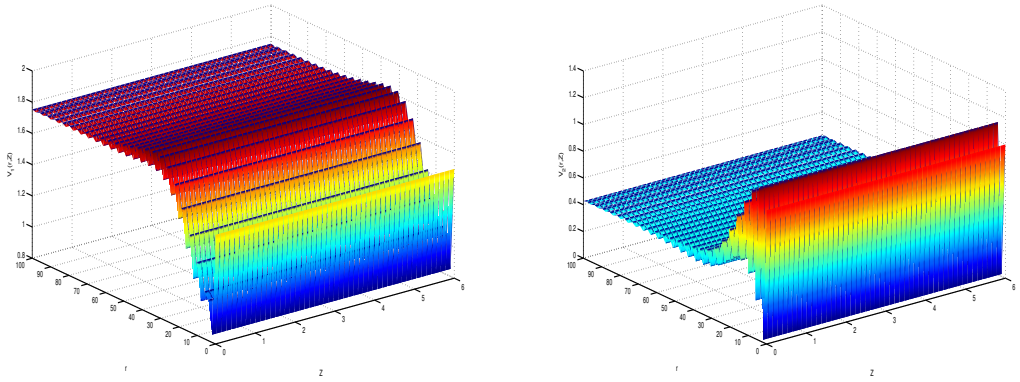

Figure 5: Dynamic behavior of the slave system (19) $\mathtt{V}_1(\mathfrak{r},\mathfrak{Z})$ and $\mathtt{V}_2(\mathfrak{r},\mathfrak{Z})$

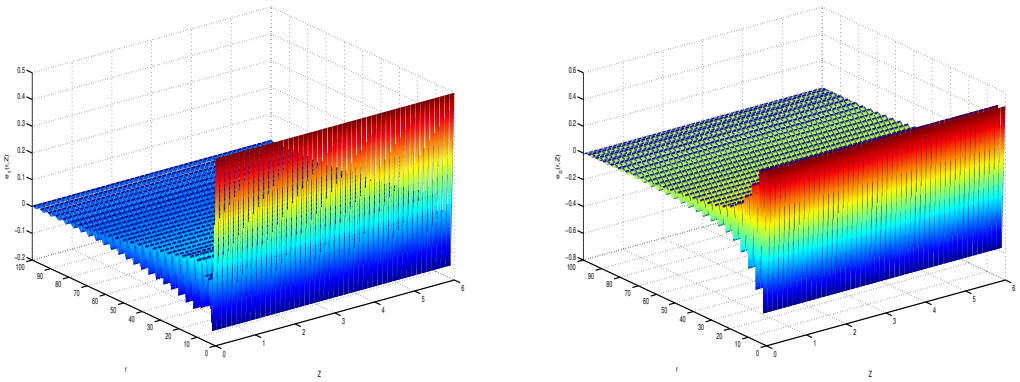

Figure 6: Dynamic behavior of the error system (21) $\mathfrak{e}_1(\mathfrak{r},\mathfrak{Z})$ and $\mathfrak{e}_2(\mathfrak{r},\mathfrak{Z})$

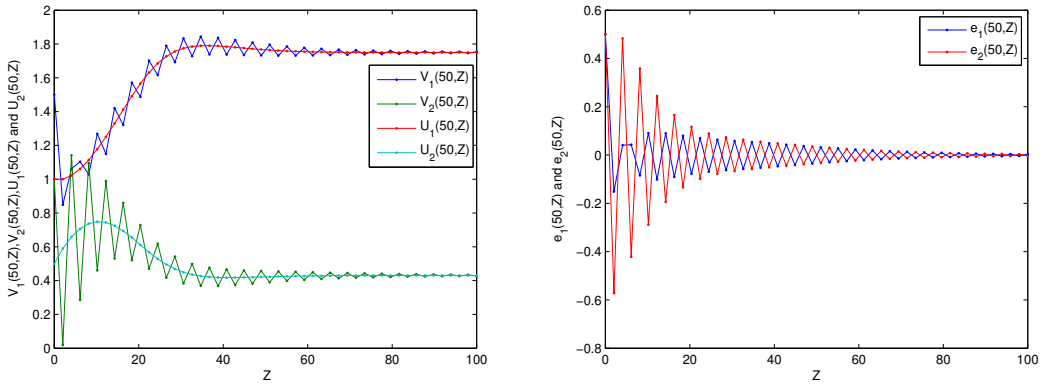

Figure 7: Solutions of the derived-response systems (1), (19), and error system (21)

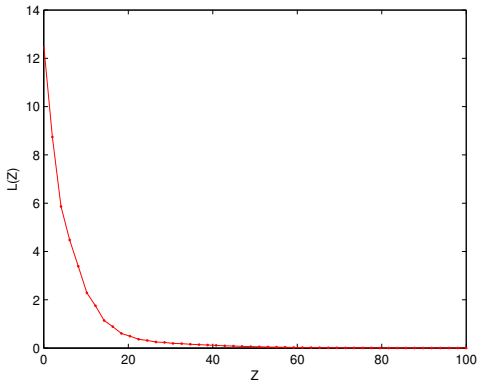

Figure 8: Estimation of the Lyapunov function $\mathtt{L}(3)$

5 Conclusion

In this study, we have demonstrated the finite-time stability of the glycolysis reaction-diffusion system at its equilibrium point. By establishing the equilibrium points of the system and determining the conditions for finite-time stability, we have shown that the system converges to equilibrium within a predetermined time frame. This is crucial for real-time control systems, where rapid stabilization is essential. Through an exhaustive analysis utilizing Lyapunov functions and Gronwall's inequality, we have confirmed that the system meets the finite-time stability criteria under specified conditions. Furthermore, the implementation of finite-time synchronization schemes ensures coherent behavior across the spatial dimensions of the system, thereby enhancing its overall performance.

References

[1] Sel'kov, E. E. Self-Oscillations in Glycolysis 1. A Simple Kinetic Model. European Journal of Biochemistry, 4, 79-86 (1968).

[2] Wolf, J., Heinrich, R. Effect of cellular interaction on glycolytic oscillations in yeast: a theoretical investigation. Biochemical Journal, 345, 321–334 (2000).

[3] Goldbeter, A. Patterns of Spatiotemporal Organization in an Allosteric Enzyme Model. Proceedings of the National Academy of Sciences of the United States of America, 70(11), 3255-3259 (1973).

[4] Zhang, L., Gao, Q., Wang, Q., Zhang, X. Simple and complex spatiotemporal structures in a glycolytic allosteric enzyme model. Biophysical Chemistry, 125, 112 (2007).

[5] Mair, T., Warnke, C., Muller, S. C. Spatio-temporal dynamics in glycolysis. Faraday Discussions, 120, 249 (2001).

[6] Abu-Ghuwaleh, M., Saadeh, R. & Qazza, A. A Novel Approach in Solving Improper Integrals. *Axioms*. **11**, 572 (2022)

[7] Ahmed, S., Qazza, A., Saadeh, R. & Elzaki, T. Conformable Double Laplace–Sumudu Iterative Method. *Symmetry*. **15**, 78 (2022)

[8] Ala'yed, O., Saadeh, R. & Qazza, A. Numerical solution for the system of Lane-Emden type equations using cubic B-spline method arising in engineering. *AIMS Mathematics*. **8**, 14747-14766 (2023)

[9] Alzahrani, A., Saadeh, R., Abdoon, M., Elbadri, M., Berir, M. & Qazza, A. Effective methods for numerical analysis of the simplest chaotic circuit model with Atangana–Baleanu Caputo fractional derivative. *Journal Of Engineering Mathematics*. **144** (2024)

[10] Alzahrani, S., Saadeh, R., Abdoon, M., Qazza, A., EL Guma, F. & Berir, M. Numerical Simulation of an Influenza Epidemic: Prediction with Fractional SEIR and the ARIMA Model. *Applied Mathematics & Information Sciences*. **18**, 1-12 (2024)

[11] Chandan, K., Saadeh, R., Qazza, A., Karthik, K., Kumar, R., Kumar, R., Khan, U., Masmoudi, A., Abdou, M., Ojok, W. & Kumar, R. Predicting the thermal distribution in a convective wavy fin using a novel training physics-informed neural network method. *Scientific Reports*. **14** (2024)

[12] Hazaymeh, A., Saadeh, R., Hatamleh, R., Alomari, M. & Qazza, A. A Perturbed Milne's Quadrature Rule for n-Times Differentiable Functions with Lp-Error Estimates. *Axioms*. **12**, 803 (2023)

[13] Saadeh, R., Abu-Ghuwaleh, M., Qazza, A. & Kuffi, E. A Fundamental Criteria to Establish General Formulas of Integrals. *Journal Of Applied Mathematics*. **2022** pp. 1-16 (2022)

[14] Saadeh, R., Ahmed, S., Qazza, A. & Elzaki, T. Adapting partial differential equations via the modified double ARA-Sumudu decomposition method. *Partial Differential Equations In Applied Mathematics*. **8** pp. 100539 (2023)

[15] Saadeh, R., Ala'yed, O. & Qazza, A. Analytical Solution of Coupled Hirota–Satsuma and KdV Equations. *Fractal And Fractional*. **6**, 694 (2022)

[16] Bagyan, S., Mair, T., Dulos, E., Boissonade, J., De Kepper, P., Muller, S. C. Glycolytic oscillations and waves in an open spatial reactor: Impact of feedback regulation of phosphofructokinase. Biophysical Chemistry, 116, 67 (2005).

[17] Lavrova, A., Bagyan, S., Mair, T., Hauser, M., Schimansky-Geier, L. Biosystems, 97, 127 (2009).

[18] Lavrova, A. I., Schimansky-Geier, L. Modeling of glycolytic wave propagation in an open spatial reactor with inhomogeneous substrate influx. Physical Review E, 79(1) (2009).

[19] Verveyko, D. V., Verisokin, A. Y., Postnikov, E. B. Mathematical model of chaotic oscillations and oscillatory entrainment in glycolysis originated from periodic substrate supply. Chaos, 27, 083104 (2017).

[20] Hamadneh, T., Hioual, A., Alsayyed, O., AL-Khassawneh, Y. A., Al-Husban, A., Ouannas, A. Local Stability, Global Stability, and Simulations in a Fractional Discrete Glycolysis Reaction–Diffusion Model. Fractal Fract., 7, 587 (2023).

[21] Ahmed, N., Ss, T., Imran, M., Rafiq, M., Rehman, M. A., Younis, M. Numerical analysis of auto-catalytic glycolysis model. AIP Advances, 9, 085213 (2019).

[22] Ouannas, A., Wang, X., Pham, V. T., Grassi, G., Huynh, V. V. Synchronization results for a class of fractional-order spatiotemporal partial differential systems based on fractional Lyapunov approach. Boundary Value Problems, 2019, 74.

[23] Eroglu, D., Lamb, J. S. W., Pereira, T. Synchronization of chaos and its applications. Contemporary Physics, 58, 207–243 (2017).

[24] Ouannas, A., Mesdoui, F., Momani, S., Batiha, I., Grassi, G. Synchronization of FitzHugh-Nagumo reaction-diffusion systems via one-dimensional linear control law. Archives of Control Sciences, 31(2), 333–345 (2021).

[25] Mesdoui, F., Ouannas, A., Shawagfeh, N., Grassi, G., Pham, V. T. Synchronization methods for the Degn-Harrison reaction-diffusion systems. IEEE Access, 8, 91829-91836 (2020).

[26] Ouannas, A., Bendoukha, S., Volos, C., Boumaza, N., Karouma, A. Synchronization of fractional hyperchaotic Rabinovich systems via linear and nonlinear control with an application to secure communications. International Journal of Control, Automation and Systems, 17, 2211–2219 (2019).

[27] Ouannas, A., Al-Sawalha, M.M. On Λ-Ψ generalized synchronization of chaotic dynamical systems in continuous-time. The European Physical Journal Special Topics, 225(1), 187–196 (2016).

[28] Ouannas, A. Co-existence of various types of synchronization between hyperchaotic maps. Nonlinear Dyn. Syst. Theory, 16, 312–321 (2016).

[29] Bendoukha, S., Ouannas, A., Wang, X., Khennaoui, A.A., Phan, V.T., Grassi, G. The co-existence of different synchronization types in fractional-order discrete-time chaotic systems with non-identical dimensions and order. Entropy, 20(9), 710 (2018).

[30] Khennaoui, A.A., Ouannas, A., Bendoukha, S., Grassi, G., Wang, X., Phan, V.T. Generalized and inverse generalized synchronization of fractional-order discrete-time chaotic systems with non-identical dimensions. Advances in Difference Equations, 2018, 1–14 (2018).

[31] Ouannas, A., Wang, X., Pham, V.T., Grassi, G., Huynh, V.V. Synchronization results for a class of fractional-order spatiotemporal partial differential systems based on fractional Lyapunov approach. Boundary Value Problems, 2019(74) (2019).

[32] Djenina, N., Ouannas, A., Batiha, I.M., Grassi, G., Pham, V.T. On the stability of linear incommensurate fractional-order difference systems. Mathematics, 8(10), 1754 (2020).

[33] Hioual, A., Oussaeif, T.E., Ouannas, A., Grassi, G., Batiha, I.M., Momani, S. New results for the stability of fractional-order discrete-time neural networks. Alexandria Engineering Journal, 61(12), 10359–10369 (2022).

[34] Saadeh, R., Abbes, A., Al-Husban, A., Ouannas, A., Grassi, G. The Fractional Discrete Predator-Prey Model: Chaos, Control and Synchronization. Fractal and Fractional, 7(2), 120 (2023).

[35] Oussaeif, T.E., Antara, B., Ouannas, A., Batiha, I.M., Saad, K.M., Jahanshahi, H. Existence and uniqueness of the solution for an inverse problem of a fractional diffusion equation with integral condition. Journal of Function Spaces, 2022 (2022).

[36] Debbouche, N., Almatroud, A.O., Ouannas, A., Batiha, I.M. Chaos and coexisting attractors in glucose-insulin regulatory system with Incommensurate fractional-order derivative. Chaos, Solitons & Fractal, 143, 110.

[37] Shatnawi, M.T., Djenina, N., Ouannas, A., Batiha, I.M., Grassi, G. Novel convenient conditions for the stability of nonlinear incommensurate fractional-order difference systems. Alexandria Engineering Journal, 61(2), 1655–1663 (2022).

[38] Ahead, I., Ouannas, A., Shafiq, M., Pham, V.T., Baleanu, D. Finite-time stabilization of a perturbed chaotic finance model. Journal of Advanced Research, 32, 1–14 (2021).

[39] Khennaoui, A.A., Almatroud, A.O., Ouannas, A., Al-sawalha, M.M., Grassi, G. An unprecedented 2-dimensional discrete-time fractional-order system and its hidden chaotic attractors. Mathematical Problems in Engineering, 2021, 1–10 (2021).

[40] Debbouche, N., Ouannas, A., Batiha, I.M., Grassi, G., Kaabar, M.K.A. Chaotic behavior analysis of a new Incommensurate fractional-order hopfield neural network system. Complexity, 2021, 1–11 (2021).

[41] Abbes, A., Ouannas, A., Shawagfeh, N., Jahanshahi, H. The fractional-order discrete COVID-19 pandemic model: stability and chaos. Nonlinear Dynamics, 111(1), 965–983 (2023).

[42] Ouannas, A., Khennaoui, A.A., Momani, S., Pham, V.T. The discrete fractional duffing system: Chaos, 0-1 test, C complexity, entropy, and control. Chaos: An Interdisciplinary Journal of Nonlinear Science, 30(8), 2020 (2020).

[43] Ouannas, A., Grassi, G., Azar, A.T., Radwan, A.G., Volos, C., Pham, V.T., Ziar, T. Dead-beat synchronization control in discrete-time chaotic systems. 2017 6th International Conference on Modern Circuits and Systems (2017).

[44] Hioual, A., Ouannas, A., Oussaeif, T.E., Grassi, G., Batiha, I.M., Momani, S. On variable-order fractional discrete neural network: solvability and stability. Fractal and Fractional, 6(2), 119 (2022).

[45] Ouannas, A., Khennaoui, A.A., Wang, X., Pham, V.T., Boulaaras, S., Momani, S. Bifurcation and chaos in the fractional form of Hénon-Lozi type map. The European Physical Journal Special Topics, 229, 2261–2273 (2020).

[46] Haddad, W.M., L'Afflitto, A. Finite-Time Stabilization and Optimal Feedback Control. IEEE Transactions on Automatic Control, 61(4), April 2016.

[47] Yang, X., Song, Q., Liu, Y., Zhao, Z. Finite-time stability analysis of fractional-order neural networks with delay. Neurocomputing, 152, 19–26 (2015).

[48] Ouannas, A., Batiha, I.M., Bekiros, S., Liu, J., Jahanshahi, H., Aly, A.A., Alghtani, A.H. Synchronization of the Glycolysis Reaction-Diffusion Model via Linear Control Law. Entropy, 23, 1516 (2020).

[49] Rao, R., Lin, Z., Ai, X., Wu, J. Synchronization of Epidemic Systems with Neumann Boundary Value under Delayed Impulse. Mathematics, 10, 2064 (2022).

[50] Corduneanu, C. Principles of Differential and Integral Equations. Allyn and Bacon, Boston (1971).

[51] Feng, Z., Xiang, Z. Finite-time stability of fractional-order nonlinear systems. Chaos, 34, 023105 (2024).

[52] Wang, L., Yang, X., Liu, H., Chen, X. Synchronization in Finite Time of Fractional-Order Complex-Valued Delayed Gene Regulatory Networks. Fractal Fract., 7, 347 (2023).

[53] Li, Y., Yang, X., Shi, L. Finite-time synchronization for competitive neural networks with mixed delays and non-identical perturbations. Neurocomputing, 185, 242–253 (2016).